2.D

Nuclear Physics **53** (1964) 577—592; © *North-Holland Publishing Co., Amsterdam*

ANGULAR MOMENTUM EFFECTS IN NEUTRON EVAPORATION

T. DARRAH THOMAS

Frick Chemical Laboratory and Princeton-Pennsylvania Accelerator Development, Princeton University, Princeton, New Jersey and Brookhaven National Laboratory, Upton, New York †

Received 18 November 1963

Abstract: The statistical model of nuclear reactions has been used to calculate the effects of angular momentum on the evaporation of neutrons. The systems considered are Po^{210} with excitation energy of 24 MeV and angular momenta up to 26 $\hbar$; At^{209} with excitation energy of 95 MeV and angular momenta up to 68.5 $\hbar$; Mn^{55} with excitation energy of 26 MeV and angular momenta up to 24.5 $\hbar$; and Rb^{79} with excitation energy of 128 MeV and angular momenta up to 73.5 $\hbar$. Quantities calculated are the average angular momentum change on evaporation of one neutron, the width for neutron emission and the average kinetic energy of the first evaporated neutron, all as a function of the angular momentum of the compound nucleus. Some approximate formulae that aid in understanding the behaviour of these quantities are discussed. A comparison is made with other similar calculations and with the existing experimental data.

1. Introduction

A number of experiments on nuclear reactions induced by heavy ions have generated considerable interest in the effects of high angular momentum on the de-excitation of a compound nucleus. Measurements have been made on neutron [1]), charged-particle [2-3]) and gamma-ray spectra [4-6]), on excitation functions for a variety of reactions including fission [7-18]) and on the angular distribution of reaction products [19-20]).

To mention one example, many (although not all) excitation functions for heavy-ion-induced reactions show a pronounced displacement towards higher energies than had been expected from the behaviour of excitation functions for proton- and alpha-particle-induced reactions [9, 12]). Kammuri and Nakasima have interpreted this effect as being due to a higher kinetic energy of the emitted neutrons resulting from the very high angular momenta of the compound nuclei [21]). On the other hand, the work of Grover [22]), Mollenauer [5]), Alexander [14]) and Morton [19]) supports the notion that the energies of the evaporated neutrons are fairly normal, and that the displacement of the excitation functions results from a gamma-ray cascade at the end of the evaporation chain. This cascade is necessary to carry off the high angular momentum left in the compound nucleus after the neutron evaporation.

Interpretation of results such as the above requires some knowledge, or at least a prediction, of the average kinetic energy of a neutron evaporated from a nucleus with high angular momentum and of the average angular momentum change during

† This work was supported in part by the U. S. Atomic Energy Commission.

such a process. It is also useful to have an idea of the width for particle emission as a function of angular momentum of the compound nucleus. It is my purpose to provide "a first extremely rough approximate orientation to the general" [23]) behaviour of these quantities.

2. Calculations

2.1. THE METHOD

The rate R at which a compound nucleus with excitation energy E_c and angular momentum J emits a particle with spin s to form a residual nucleus with excitation energy E_f and angular momentum j is given by the following expression †:

$$R\mathrm{d}E_f = \frac{1}{\hbar}\frac{\Omega(E_f, j)}{\Omega(E_c, J)}\sum_{S=|j-s|}^{j+s}\sum_{l=|J-S|}^{J+S} T_l\,\mathrm{d}E_f. \tag{2.1}$$

Here, T_l is the transmission coefficient for the lth partial wave of the emitted particle and S is the channel spin, defined as $S = s+j$. The spin dependent level density is assumed to be

$$\Omega(E, J) = \frac{(2J+1)}{\pi^{\frac{1}{4}}(2c\tau)^{\frac{3}{4}}}\exp\left[-(J+\tfrac{1}{2})^2/2c\tau\right]\omega(E). \tag{2.2}$$

The nuclear temperature τ is defined by the expresssion

$$1/\tau = \mathrm{d}\log\omega(E)/\mathrm{d}E, \tag{2.3}$$

where ω is the total density of states. The quantity $c\hbar^2$ is the nuclear moment of inertia $\mathscr{I}$. We assume that c does not vary with excitation energy.

The particular significance attached to c and τ, namely that $c\hbar^2$ is the moment of inertia and that τ is the nuclear temperature, is that used by Lang and Le Couteur [25]). It is perhaps more nearly correct to use the thermodynamic temperature t (see eq. (2.5) below) rather than the nuclear temperature ††. However, at the energies involved in these calculations, the difference between t and τ is not significant.

If we assume that the nucleus is a Fermi gas, then the density [25]) of states

$$\omega(E) = B(E+t)^{-5/4}\exp\left[2(aE)^{\frac{1}{2}}\right], \tag{2.4}$$

where B is a constant, a is the "level density parameter". The thermodynamic nuclear temperature t and the excitation energy E are related by the following expression:

$$E = at^2 - t. \tag{2.5}$$

Once we have chosen a, c and some appropriate model for calculating transmission coefficients, we can use eq. (2.1) to calculate the spin and energy spectrum of residual nuclei resulting from the evaporation of some particle from a given compound

† A derivation of this expression is sketched in ref. [24]).

†† A brief discussion of this point is given in the preceding paper.

nucleus. This spectrum integrated over final energies and summed over final angular momenta gives $\Gamma/\hbar$, where Γ is the width for particle emission. The same spectrum summed over final angular momenta and subsequently averaged over final energies gives the average excitation energy of the residual nucleus and, hence, the average kinetic energy $\bar{\varepsilon}$ of the emitted particle. Similarly, the spectrum integrated over final energies and averaged over final angular momenta gives the average angular momentum of the residual nucleus, and, hence, the average change in angular momentum Δ on evaporation of a particle.

2.2. THE PARAMETERS

Calculations were performed for four different systems of compound nuclei; Po^{210}, as if produced by 30 MeV alpha particles incident on Pb^{206}; At^{209}, as if

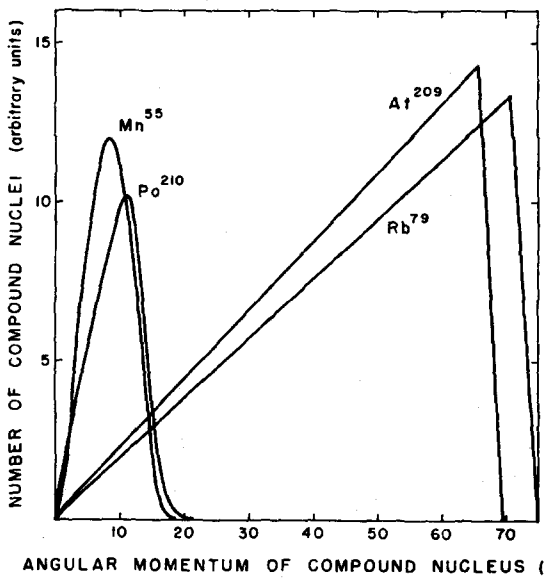

Fig. 1. Angular momentum distribution of the four compound nuclei considered. If the level density goes to zero for $E < E_J$ then the Rb^{79} curve should cut off at $J = 70.5\,\hbar$ for $\mathcal{I} = \mathcal{I}_{rigid}$ and at $J = 38.5\,\hbar$ for $\mathcal{I} = 0.3\,\mathcal{I}_{rigid}$ and that for Mn^{55} at $J = 12.5\,\hbar$ for $\mathcal{I} = 0.3\,\mathcal{I}_{rigid}$.

produced by 120 MeV carbon ions incident on Au^{197}; Mn^{55}, as if produced by 20 MeV alpha particles incident on V^{51}; and Rb^{79}, as if produced by 160 MeV oxygen ions incident on Cu^{63}. The initial spin distribution of the compound nuclei formed in the heavy-ion-induced reactions were calculated under the assumption that $T_l = 1$ up to the classical maximum of l and 0 beyond. In determining the classical maximum of l, the radius parameter $r_0 = 1.5$ fm was used. For the alpha-particle-induced reactions the initial spin distributions are based on the transmission coefficients given by Huizenga and Igo [26,27]). Fig. 1 shows the distributions for the four systems.

Neutron transmission coefficients, using a square-well black nucleus model † with $r_0 = 1.5$ fm, were calculated. This rather large value of r_0 is necessary if the square-well model is to given realistic values of the cross section.

A value of $A/12$ MeV^{-1} for the level density parameter a, is in agreement with the prediction of the Fermi gas model [28]). This value also results from an analysis of evaporation spectra taking into account that the angular momentum dependence of the level density is given by eq. (2.2) ††.

It is not clear what value to use for the moment of inertia $\mathscr{I}$ of the excited nucleus. At sufficiently high energies the moment of inertia is expected to be the rigid body moment $\mathscr{I}_{\text{rigid}}$. A variety of experiments have given values ranging from about 0.3 rigid body to rigid body †††. Therefore, calculations were performed with $\mathscr{I} = 0.3\ \mathscr{I}_{\text{rigid}}$, $\mathscr{I} = \mathscr{I}_{\text{rigid}}$, and $\mathscr{I} = 10^4 \mathscr{I}_{\text{rigid}}$. The last of these is to show what happens if we assume that $\Omega(E, J) \propto 2J+1$. In calculating the rigid body moment of inertia, the values of r_0 given by Hofstadter [29]) have been used. These values, 1.2 fm for $A \lesssim 100$ and slightly greater for $A \gtrsim 100$, give the correct value for the mean-square radius as determined by electron scattering experiments.

For a given excitation energy eq. (2.2) predicts a finite level density for any angular momentum, no matter how high. However, for each angular momentum J, there must, in fact, be an energy E_J, below which there are no levels with that angular momentum. For that particular J, the level density should be 0 for energies less than E_J.

Sperber [30]) and Grover [22]) have investigated the relationship between E_J and J and have both come to the conclusion that

$$E_J \approx J(J+1)\hbar^2/2\mathscr{I}. \tag{2.6}$$

In Grover's analysis, there is an additive term that is important for low values of J. He concludes, with some qualifications, that the moment of inertia appearing in eq. (2.6) is the same as that used in the level density expression eq. (2.2). It is by no means certain, however, that the quantities are necessarily the same; this is a point awaiting experimental investigation. Sperber has considered four different nuclear models and concludes that $\mathscr{I}$, as used in eq. (2.6), is within about a factor of 2 of the rigid body moment. It should be noted that, at this time, there is no experimental verification of eq. (2.6).

With these qualifications in mind, a series of calculations have been performed under the assumption that $\Omega(E, J) = 0$ if $E < E_J$ and that the moment of inertia defining E_J is the same as that used to calculate the level density. Ideally, it would be better to use a function that went more smoothly to 0 at $E = E_J$, such as that proposed by Lang [31]), but the approximation used is good enough for the present purpose.

† See ref. [28]), chapter 8.

†† See the preceding paper.

††† For a short list of references on the moment of inertia, see the preceding paper.

3. Results and Discussion

The results of the calculations described above are shown in figs. 2-4. In each case the solid curves were calculated under the assumption that the level density is given by eq. (2.2) for all values of the excitation energy and angular momentum, and the dashed curves under the assumption that the level density is 0 for $E < E_J$. For At^{209} and Po^{210} there is no difference between the results based on the two assumptions. For Mn^{55} and Rb^{79} the dashed curves do not extend to as high angular momenta as do the solid ones because of the absence of levels in the compound nucleus with high angular momentum.

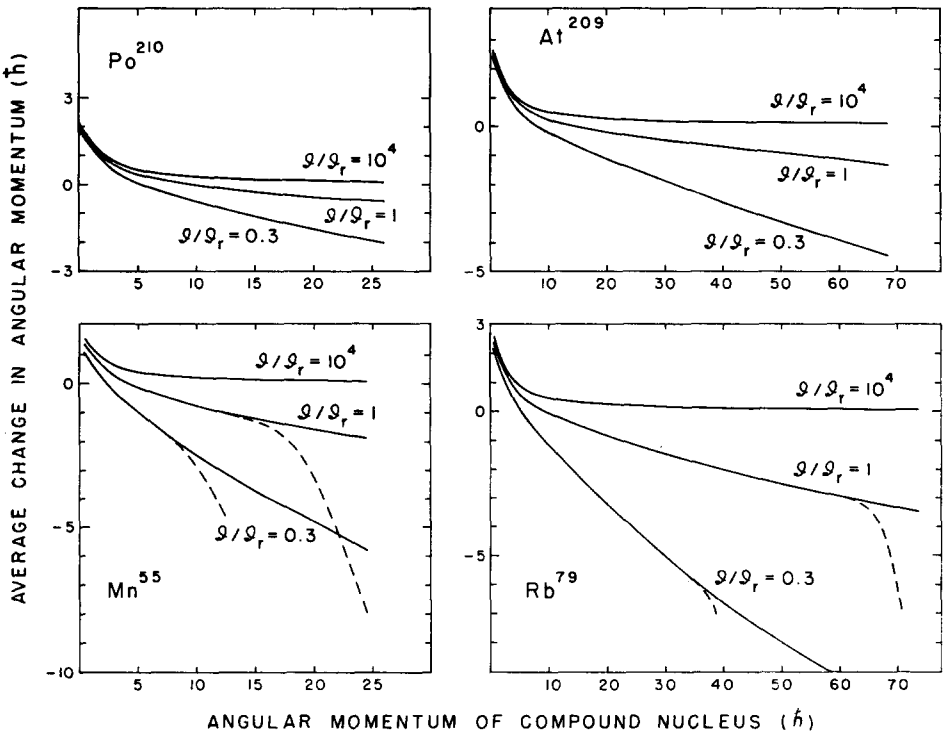

Fig. 2. The average change in angular momentum on evaporation of one neutron as a function of the angular momentum of the compound nucleus. The solid curves are calculated assuming that the level density is given by eq. (2.2) for all angular momenta and the dashed curves assuming that the level density goes to zero for $E < E_J$.

3.1. THE AVERAGE CHANGE IN ANGULAR MOMENTUM

Fig. 2 shows the average change in angular momentum Δ upon evaporation of one neutron as a function of the angular momentum of the compound nucleus. The qualitative features of these curves are easily understood. If $d\Omega/dJ$ is positive the angular momentum will, on the average, increase upon evaporation of a neutron;

if $d\Omega/dJ$ is negative the angular momentum will decrease. In fact, all of the solid curves of fig. 2 can be fit to within about 10 percent by the relationship

$$\Delta = G\, d \log \Omega/dJ \tag{3.1}$$

$$= G\left\{\frac{1}{J+\frac{1}{2}} - \frac{J+\frac{1}{2}}{c\tau}\right\}. \tag{3.2}$$

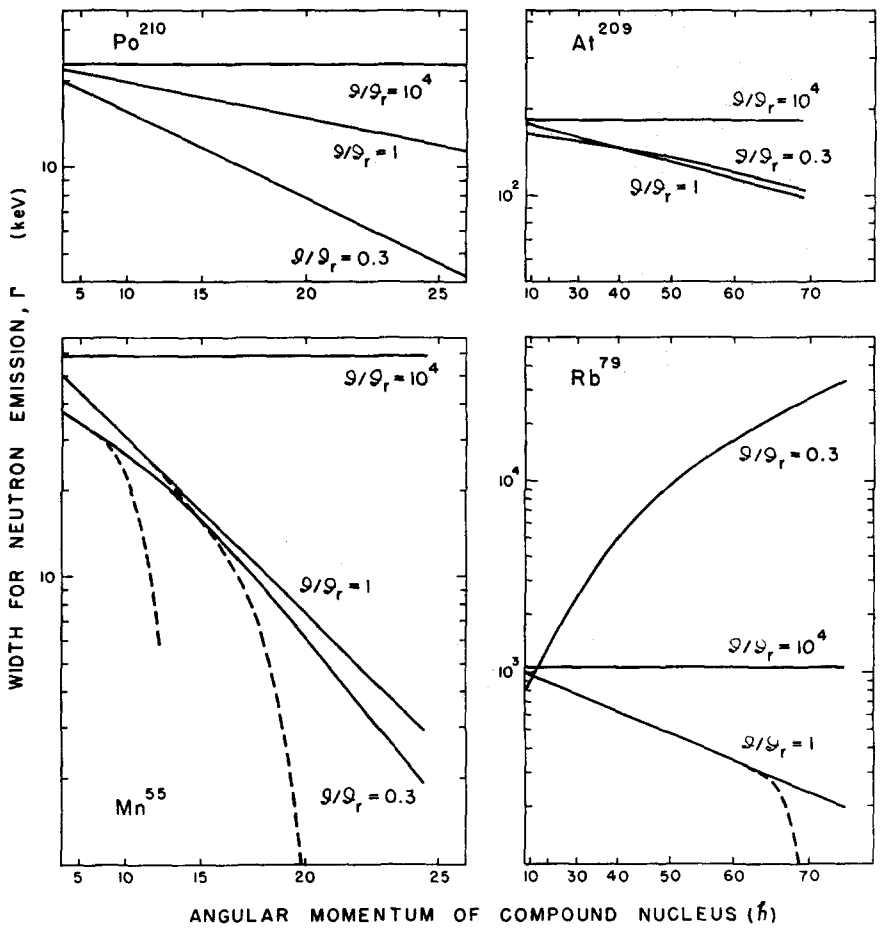

Fig. 3. The width for neutron emission as a function of the angular momentum of the compound nucleus. The solid curves are calculated assuming that the level density is given by eq. (2.2) for all angular momenta and the dashed curves assuming that the level density goes to zero for $E < E_J$.

The constant of proportionality G is empirically about 5 for the two high energy cases, At^{209} and Rb^{79}, and about 2 for the two low-energy cases. Although it is not surprising that there is a dependence of Δ on this derivative, it is not obvious that there should be such a simple relationship.

In the case of the dashed curves, the unavailability of levels of high angular momentum in the residual nucleus requires a large negative Δ for compound nuclei of high angular momenta.

3.2. THE WIDTH FOR NEUTRON EMISSION

In fig. 3 is plotted the logarithm of the width for neutron emission Γ (calculated using eq. (2.1)) as a function of the angular momentum of the compound nucleus J. The numbers on the abscissa give the value of J, but the spacing is proportional to $(J+\frac{1}{2})^2$.

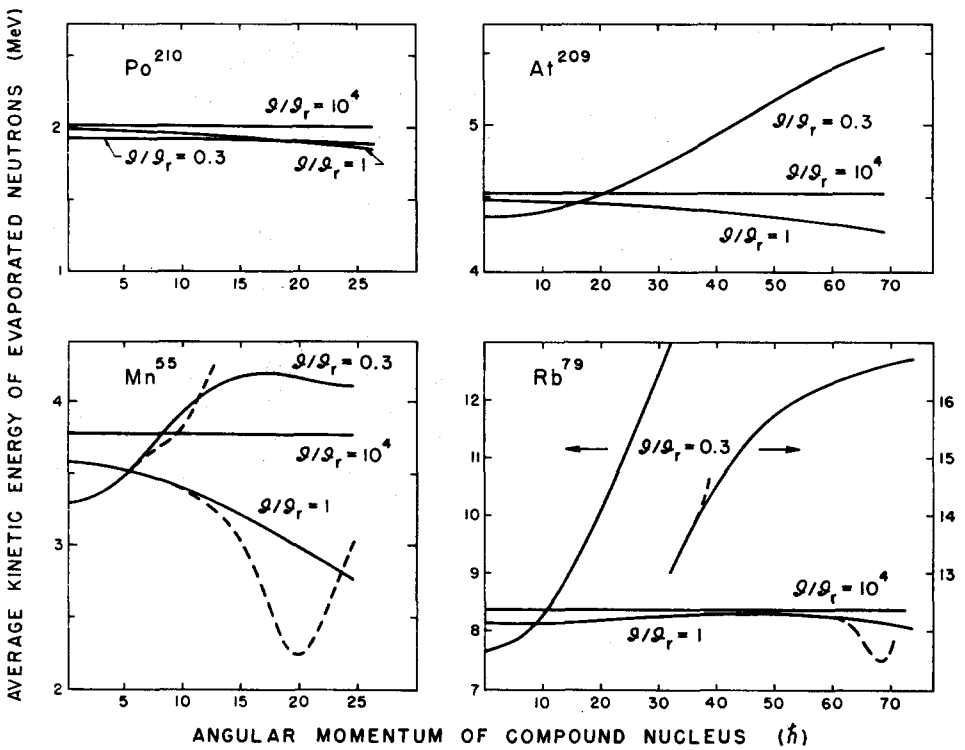

Fig. 4. The average kinetic energy of the first evaporated neutron as a function of the angular momentum of the compound nucleus. The solid curves are calculated assuming that the level density is given by eq. (2.2) for all angular momenta and the dashed curves assuming that the level density goes to zero for $E < E_f$.

On the basis of a simplifying assumption we can derive an approximate expression for the behaviour of Γ with J. We substitute eq. (2.2) into expression (2.1) and rewrite as follows:

$$R\,\mathrm{d}E_\mathrm{f} = \frac{1}{\hbar}\frac{(2j+1)\exp\left[-(j+\frac{1}{2})^2/2c\tau_\mathrm{f}\right]}{(2J+1)\exp\left[-(J+\frac{1}{2})^2/2c\tau_\mathrm{c}\right]}\, I'(E_\mathrm{c}, E_\mathrm{f}) \sum_{S=|j-s|}^{j+s} \sum_{l=|J-S|}^{J+S} T_l\,\mathrm{d}E_\mathrm{f}. \qquad (3.3)$$

Here $I'(E_\mathrm{c}, E_\mathrm{f})$ represents all of the factors that depend only on the initial and final energies. We make the simplifying assumption that the exponential term in the

numerator of eq. (3.3) does not vary rapidly with either final energy or final angular momentum and set it equal to its average value. Then, summing over final angular momenta we have

$$R\mathrm{d}E_\mathrm{f} = \frac{1}{\hbar}\frac{\exp\left[-(j+\frac{1}{2})^2/2c\bar{\tau}_\mathrm{f}\right]}{(2J+1)\exp\left[-(J+\frac{1}{2})^2/2c\tau_\mathrm{c}\right]} I'(E_\mathrm{c}, E_\mathrm{f}) \sum_{j=0}^{\infty}(2j+1)\sum_{S=|j-s|}^{j+s}\sum_{l=|J-S|}^{J+S} T_l \mathrm{d}E_\mathrm{f}. \tag{3.4}$$

The symbols j and $\bar{\tau}_\mathrm{f}$ refer to the average values of j and τ_f. Reversing the order of summation and carrying out the sums over j and S, we get

$$R\mathrm{d}E_\mathrm{f} = \frac{1}{\hbar}(2s+1)\exp\left[-\frac{(j+\frac{1}{2})^2}{2c\bar{\tau}_\mathrm{f}} + \frac{(J+\frac{1}{2})^2}{2c\tau_\mathrm{c}}\right] I'(E_\mathrm{c}, E_\mathrm{f})\sum_{l=0}^{\infty}(2l+1)T_l\mathrm{d}E_\mathrm{f}. \tag{3.5}$$

Now we integrate over final energies and multiply by $\hbar$ to obtain

$$\Gamma = I(E_\mathrm{c})\exp\left[-\frac{(j+\frac{1}{2})^2}{2c\bar{\tau}_\mathrm{f}} + \frac{(J+\frac{1}{2})^2}{2c\tau_\mathrm{c}}\right] \tag{3.6}$$

where $I(E_\mathrm{c})$ represents the integral over the energy dependent terms. With the relationship $\Delta = j - J$ we can re-arrange eq. (3.6) to give

$$\Gamma = I(E_\mathrm{c})\exp\left\{\frac{1}{2c\bar{\tau}_\mathrm{f}}\left[-(J+\tfrac{1}{2})^2\left(1-\frac{\bar{\tau}_\mathrm{f}}{\tau_\mathrm{c}}\right) - (2J+1)\Delta - \Delta^2\right]\right\}. \tag{3.7}$$

Finally, substituting eq. (3.2) into expression (3.7) and ignoring a term in $(J+\frac{1}{2})^{-2}$, which will be important only for small values of J, we have

$$\Gamma \propto \exp\left\{-\frac{(J+\frac{1}{2})^2}{2c\bar{\tau}_\mathrm{f}}\left[\left(1-\frac{\bar{\tau}_\mathrm{f}}{\tau_\mathrm{c}}\right) - \frac{2G}{c\bar{\tau}_\mathrm{f}} + \frac{G^2}{(c\bar{\tau}_\mathrm{f})^2}\right]\right\}. \tag{3.8}$$

Noting that $(1-\bar{\tau}_\mathrm{f}/\tau_\mathrm{c})$ is positive, we see that plots such as those in fig. 3 should have close to zero slope for very large values of the moment of inertia, should be linear with negative slope for moderately large values, should have positive slope for small values, and negative slope again for extremely small values. The curves in fig. 3 show this expected behaviour and indicate that the last term in eq. (3.8) is probably not important.

If we assume a constant temperature level density expression, then $(1-\bar{\tau}_\mathrm{f}/\tau_\mathrm{c}) = 0$ and we expect Γ to increase with τ even for large moments of inertia. This effect is illustrated in fig. 5(a), which shows the results of an exact calculation using eq. (2.1) for At^{209} with $\mathscr{I} = \mathscr{I}_{\mathrm{rigid}}$ and with

$$\Omega \propto \exp E/T, \tag{3.9}$$

where $T = 2.2$ MeV.

3.3. THE AVERAGE KINETIC ENERGY OF EVAPORATED NEUTRONS

Fig. 4 illustrates how the average kinetic energy of an evaporated neutron varies as a function of initial angular momentum. We can understand the qualitative features of these curves with a simple classical model.

Consider the evaporation of particles from a non-rotating nucleus and assume that all particles are emitted along a radius (i.e. $l = 0$). They will have an average energy 2τ, where τ is the temperature of the nucleus remaining after the evaporation. If the nucleus is rotating, then each particle will also have a component of velocity tangential to the surface and equal to the surface velocity.

If R is the radius of the nucleus, $J\hbar$ its angular momentum and $\mathscr{I}$ its moment of inertia, then the surface velocity of any point

$$v = RJ\hbar(\sin\theta)/\mathscr{I}, \tag{3.10}$$

where θ is the angle between the radius locating the particular point and the direction of the angular momentum.

The resultant energy of the emitted particle is given as

$$\varepsilon = 2\tau_J + mR^2J^2\hbar^2(\sin^2\theta)/2\mathscr{I}^2, \tag{3.11}$$

where m is the mass of the particle. The quantity τ_J is the temperature of the rotating nucleus and is, in general, less than the temperature of a non-rotating nucleus with the same excitation energy. For the rotating nucleus part of the energy exists as rotational energy and only the remainder is heat.

Averaging over θ gives

$$\bar{\varepsilon} = 2\tau_J + \tfrac{2}{3}\frac{mR^2}{\mathscr{I}}E_{\mathrm{rot}}, \tag{3.12}$$

where

$$E_{\mathrm{rot}} = J^2\hbar^2/2\mathscr{I}. \tag{3.13}$$

Ericson [32]) has derived a formula that is identical in form to eq. (3.12) but his coefficient of the second term is $\frac{4}{3}$ rather than $\frac{2}{3}$.

We can estimate the first term in eq. (3.12) in a manner similar to that used by Broek [1]), namely

$$1/\tau_J = \mathrm{d}\ln\omega(E, J)/\mathrm{d}E, \tag{3.14}$$

where $\omega(E, J)$ is the density of states with angular momentum J

$$\omega(E, J) = (2J+1)\Omega(E, J). \tag{3.15}$$

Recalling eq. (2.2), which gives the angular momentum dependence of the level density $\Omega(E, J)$, we can show that

$$\frac{1}{\tau_J} = \frac{1}{\tau} + \left(\frac{(J+\frac{1}{2})^2}{2c\tau} - \tfrac{3}{2}\right)\frac{\mathrm{d}\ln\tau}{\mathrm{d}E}, \tag{3.16}$$

or

$$\tau_J = \tau \Big/ \left(1 + \left[\frac{(J+\frac{1}{2})^2}{2c\tau} - \tfrac{3}{2}\right]\frac{\mathrm{d}\tau}{\mathrm{d}E}\right) \tag{3.17}$$

where τ is the usual nuclear temperature, given by eq. (2.3). Using the approximate expression $\tau = (E/a)^{\frac{1}{2}}$, we can rewrite eq. (3.17) as follows:

$$\tau_J \approx \tau \Big/ \left(1 + \frac{E_{\text{rot}}}{2E} - \frac{3}{4(aE)^{\frac{1}{2}}}\right). \tag{3.18}$$

This expression shows the expected decrease as the angular momentum increases.

For $E_{\text{rot}} < E$, we can expand eq. (3.18) to give

$$\tau_J \approx \tau - \frac{E_{\text{rot}}}{2(Ea)^{\frac{1}{2}}} + \frac{3}{4a}. \tag{3.19}$$

Dropping the last term, which is constant, and substituting eq. (3.19) into expression (3.12)

$$\bar{\varepsilon} = 2\tau + E_{\text{rot}}\left(\tfrac{2}{3}\frac{mR^2}{\mathscr{I}} - \frac{1}{(Ea)^{\frac{1}{2}}}\right). \tag{3.20}$$

From this approximate relationship we can see that for small values of the excitation energy and large values of the moment of inertia the average kinetic energy

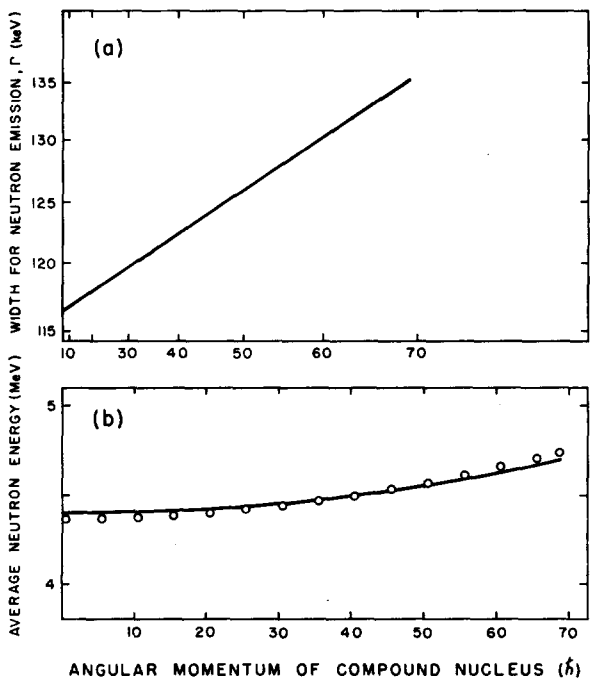

Fig. 5. (a) The width for neutron emission for At^{209} as a function of angular momentum of the compound nucleus assuming the nuclear temperature is constant and equal to 2.2 MeV. (b) The average kinetic energy of the first neutron evaporated from the same system under the same assumptions. The open circles are the results of an exact calculation using eqs. (2.1) and (2.2). The solid curve is based on eq. (3.12) with τ_J held constant.

decreases with increasing angular momentum. For large values of the excitation energy and small values of the moment of inertia the reverse is true. The curves in fig. 4 show the expected behaviour.

If we assume a constant temperature nucleus, then we predict that the kinetic energy will always increase with angular momentum regardless of the moment of inertia. Exact calculations show this to be the case, as is illustrated in fig. 5(b) for At^{209}. The points are the results of the exact calculation and the curve is the prediction of eq. (3.12), with τ_J held constant.

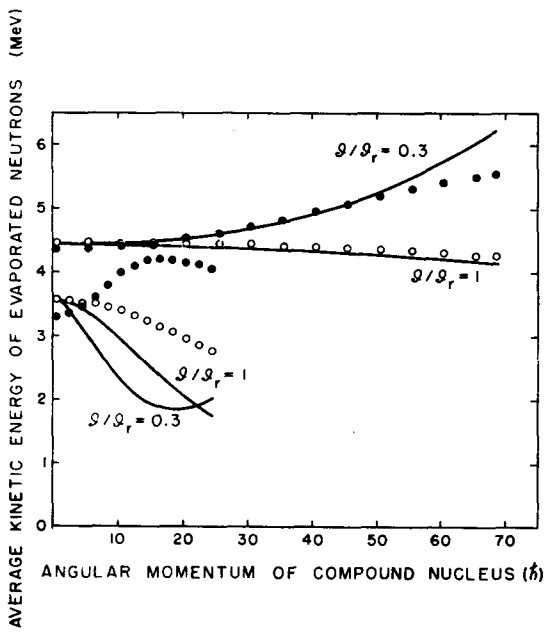

Fig. 6. A comparison of exact results (points) based on eqs. (2.1) and (2.2) and approximate calculations based on eq. (3.12) (curves). The upper set of curves are for At^{209} and the lower set for Mn^{55}. Open circles are based on the rigid body moment of inertia and solid circles on a moment equal to 0.3 the rigid body value.

Fig. 6 shows comparisons between the predictions of eq. (3.12) and several of the solid curves of fig. 4. The upper set of curves are for At^{209} and the lower set for Mn^{55}; open circles are based on the rigid body moment of inertia and solid circles on a moment equal to 0.3 the rigid body value. The curves are based on eq. (3.12). For the approximate calculations, shown in figs. 5 and 6, values of τ_J given by (3.18) were used (except for fig. 5, where $\tau_J = 2.2$ MeV), $R = 1.5A^{\frac{1}{3}}$ fm, and moments of inertia were calculated in the manner described above (subsect. 2.2). We see from fig. 6 that the approximate formula works remarkably well at high excitation energies and fairly high moments of inertia, but fails badly at low excitation energies and low moments of inertia.

The dashed curves of fig. 4 are initially lower than the solid curves because of the elimination of low-energy states of a given angular momentum and hence the elimination of high kinetic energy neutrons from the spectra. At higher initial angular momenta, however, there are no levels in the final nucleus that can be populated by neutrons emitted with low orbital angular momentum. The higher l values necessary require higher kinetic energies and therefore the dashed curves in fig. 4 increase with increasing angular momentum for high values of the angular momentum.

3.4. AVERAGES OVER THE INITIAL SPIN SPECTRA

Since any experiment measures a quantity representing an average over the initial angular momentum spectrum of the compound nucleus, it is interesting to evaluate

TABLE 1

Average neutron kinetic energy $\bar{\varepsilon}$ and average change in angular momentum Δ due to the emission of one neutron

$\mathcal{I}/\mathcal{I}_{\text{rigid}}$	$\bar{\varepsilon}$(MeV)	$\Delta(\hbar)$
Po^{210}		
1.0	1.96	0.09
1.0 [a])	1.96	0.09
0.3	1.92	−0.46
0.3 [a])	1.92	−0.46
10^4	2.01	0.36
At^{209}		
1	4.37	−0.81
1.0 [a])	4.37	−0.81
0.3	5.06	−2.93
0.3 [a])	5.06	−2.93
10^4	4.53	0.14
Mn^{55}		
1.0	3.43	−0.51
1.0 [a])	3.41	−0.52
0.3	3.77	−1.96
0.3 [a])	3.70	−2.07
10^4	3.77	0.32
Rb^{79}		
1.0	8.28	−2.35
1.0 [a])	8.15	−2.56
0.3	14.74	−7.54
0.3 [a])	11.62	−4.94
10^4	8.39	0.13

Averages are taken over the initial spin distributions of fig. 1

[a]) Calculated under the assumption that the level density is 0 for $E < E_J$.

these averages. Table 1 gives the neutron kinetic energy and the change in angular momentum averaged over the assumed initial distributions of angular momentum given in fig. 1.

4. Comparison with Other Work

4.1. OTHER CALCULATIONS

Calculations similar to those described here have been performed by Pik-Pichak [33]), Kammuri and Nakasima [21]) and Broek [1]). Pik-Pichak has considered a rather different model and a constant nuclear temperature. As we would expect from the above considerations, he finds that Γ and $\bar{\varepsilon}$ increase with increasing angular momentum. In fact, exact calculations with eq. (2.1) using the same parameters that Pik-Pichak has used yield results that are qualitatively the same as his but that give values of Γ that are more than a factor of ten smaller than his.

Kammuri and Nakasima [21]) have concerned themselves specifically with the variation of the neutron kinetic energy with angular momentum. For Zn^{65} at an excitation energy of 60 MeV and with moment of inertia 0.25 $\mathscr{I}_{\text{rigid}}$ they find an increase in the most probable neutron energy from 4 to 14 MeV as the initial angular momentum goes from $4\hbar$ to 28 $\hbar$. As we have seen, this is the expected behaviour for a low moment of inertia and a high initial energy. The effects they have calculated are enhanced by the fact that in addition to using a small moment of inertia they also used $r_0 = 2.2$ fm in determining the transmission coefficients for the outgoing neutrons.

Broek [1]) has calculated the temperature of neutrons emitted from the average compound nucleus produced when 160 MeV oxygen ions are incident on aluminium, nickel, copper and gold. For each case he calculates a lowering of the temperature because of the angular momentum. Since he uses a fairly large moment of inertia (rigid body with $r_0 = 1.5$ fm) this result is reasonable.

4.2. EXPERIMENTAL RESULTS

4.2.1. *Neutron evaporation spectra*

The most direct information is, at first glance, the spectra measured by Broek for neutrons produced in O^{16} ion bombardment of aluminium, nickel, copper and gold [1]). However, in the irradiations of gold at least 90% of the compound nuclei formed undergo fission with the result that the observed spectra are strongly weighted with post-fission neutrons [11]). For the light targets as much as 50% of the interactions result in some kind of direct interaction in which an excited nucleus with somewhat less than the full energy and full angular momentum is formed [2]). Thus, average energies determined from Broek's work with light element targets represent a lower limit to the energy averaged over all the neutrons emitted in a given compound nucleus de-excitation.

For the bombardments of copper, Broek's results indicate an average neutron energy of 3.4 MeV. Simonoff and Alexander have concluded that this average varies as the square root of the initial excitation energy [20]); if this is the case, then the average kinetic energy of neutrons emitted from the initial compound nucleus is about 1.5 times the energy averaged over all of the successive compound nuclei, or 5.1 MeV.

This value is substantially lower than any of the values given in table 1 for this system. The inclusion of temperature lowering due to half of the interactions resulting in direct interactions is not able to account for the discrepancy. It is possible that because the initial compound nucleus is quite neutron deficient, no neutrons are emitted until after some charged particle evaporation has taken place, causing cooling of the nucleus.

4.2.2. *Measurements of recoil properties and excitation functions*

Less direct than the measurement of evaporation spectra but more specific is the work of Alexander and Simonoff [14, 20]). By studying the excitation functions for production of particular products and by determining the recoil properties of these products they are able to focus attention on one reaction path out of the many that are present in a heavy-ion-induced reaction.

A typical system studied by Alexander and Simonoff [14]) is the Dy^{156} compound nucleus, with an excitation energy of 87 MeV and an average angular momentum of 46 $\hbar$. Their angular distribution studies indicate that the average energy of the first neutron $\bar{\varepsilon}$ is 4.2 ± 0.4 MeV. Their excitation function studies suggest that

$$\bar{\varepsilon} = 2.0 - 0.47\Delta \pm 1.5 \text{ MeV}.$$

To see what would be predicted for this system, three calculations were performed, assuming that $\mathscr{I} = \mathscr{I}_{\text{rigid}}$, $0.5\mathscr{I}_{\text{rigid}}$, and $0.3\mathscr{I}_{\text{rigid}}$ and that the level density is 0 for $E < E_J$. (In this case the results do not depend very strongly on whether or not the last of these assumptions is made.) The results are summarized in table 2.

TABLE 2

Quantities of interest in the de-excitation of Dy^{156}

$\mathscr{I}/\mathscr{I}_{\text{rigid}}$	$\bar{\varepsilon}_{\text{calc}}$ (MeV)	Δ ($\hbar$)	$\bar{\varepsilon}_{\text{expt}}$ [a]) (MeV)	$\bar{\varepsilon}_{\text{expt}}$ [b]) (MeV)
1	4.71	−1.0	2.5	4.2
0.5	5.04	−2.3	3.1	4.2
0.3	5.81	−3.2	3.5	4.2

[a]) From excitation functions, ref. [14]).
[b]) From angular distributions, ref. [14, 20]).

Looking at these figures, we again find, that the calculated values are higher than the experimental ones. The limits of error (± 1.5 MeV) on the numbers in the next to last column are too big for us to draw any definite conclusion from the agreement or lack of agreement between them and the numbers in the last column.

5. Conclusion

From what has been presented, we can see that the general dependence of the calculated quantities Δ, Γ and $\bar{\varepsilon}$ on the angular momentum of the compound nucleus

can be understood with the help of approximate formulae. However, the results also indicate that the approximate formulae are probably of little value for predicting these quantities.

For light elements and low energies it is necessary to take account of the fact that for a given angular momentum J there are no levels below a certain energy E_J. Figs. 2-4 and table 1 give an indication of the different results that can be obtained, depending on whether we do or do not consider this effect.

The calculated average kinetic energies are somewhat higher than those that have been estimated from experimental work. A value of $a = \frac{1}{8}A$ rather than $a = \frac{1}{12}A$ in the calculations should bring these into closer agreement.

I would like to express my appreciation to Dr. J. Robb Grover for many helpful comments and discussions and to Mrs. Arlene Larsen for help in the programming of this problem for the computer.

References

1) H. W. Broek, Phys. Rev. **124** (1961) 233
2) W. J. Knox, A. R. Quinton and C. E. Anderson, Phys. Rev. **120** (1960) 2120
3) H. C. Britt and A. R. Quinton, Phys. Rev. **124** (1961) 877
4) V. A. Karnaukhov and Yu. Ts. Oganesyan, JETP **38** (1960) 1339; JETP **11** (Soviet Physics) (1960) 964
5) J. F. Mollenauer, Phys. Rev. **127** (1962) 867
6) Yu. Ts. Oganesyan, Yu. V. Lobanov, B. N. Lobanov, B. N. Markov and G. N. Flerov, JETP **44** (1963) 1171; JETP (Soviet Physics) **17** (1963) 791
7) S. A. Baraboshkin, A. S. Karamyan and G. N. Flerov, JETP **32** (1957) 1294; JETP (Soviet Physics) **5** (1957) 1055
8) T. Sikkeland, S. G. Thompson and A. Ghiorso, Phys. Rev. **112** (1958) 543
9) A. S. Karamyan, Yu. B. Gerlit and B. F. Myasoedov, JETP **36** (1959) 621; JETP (Soviet Physics) **9** (1959) 431
10) V. V. Volkov, L. I. Gusyeva, A. S. Pasyouk, N. I. Tarantin and K. V. Filippova, JETP **36** (1959) 762; JETP (Soviet Physics) **9** (1959) 536
11) T. D. Thomas, G. E. Gordon, R. M. Latimer and G. T. Seaborg, Phys. Rev. **126** (1962) 1805
12) G. R. Choppin and T. J. Klingen, Phys. Rev. **130** (1963) 1990, 1996
13) J. M. Alexander and G. N. Simonoff, Phys. Rev. **130** (1963) 2383
14) J. M. Alexander and G. N. Simonoff, Phys. Rev. **133** (1964) B93
15) V. A. Druin, S. M. Polikanov and G. N. Flerov, JETP **32** (1957) 1298; JETP (Soviet Physics) **5** (1957) 1059
16) S. M. Polikanov and V. A. Druin, JETP **36** (1959) 744; JETP (Soviet Physics) **9** (1959) 522
17) T. Sikkeland, A. E. Larsh and G. E. Gordon, Phys. Rev. **123** (1961) 2112
18) V. E. Viola, Jr. and T. Sikkeland, Phys. Rev. **128** (1962) 767
19) J. R. Morton, III, G. R. Choppin and B. G. Harvey, Phys. Rev. **128** (1962) 265
20) G. N. Simonoff and J. Alexander, Phys. Rev. **133** (1964) B104
21) T. Kammuri, Prog. Theor. Phys. **25** (1961) 235;
T. Kammuri and R. Nakasima, in Proc. Second Conf. on Reactions Between Complex Nuclei (John Wiley and Sons, New York, 1960) paper E-8, p. 301
22) J. R. Grover, Phys. Rev. **127** (1962) 2142
23) J. M. Blatt and V. F. Weisskopf, Theoretical nuclear physics (John Wiley and Sons, New York, 1952) p. 372

24) T. D. Thomas, Nuclear Physics **53** (1964) 558
25) J. M. B. Lang and K. J. Le Couteur, Proc. Phys. Soc. **67A** (1954) 586
26) J. R. Huizenga and G. J. Igo, Nuclear Physics **29** (1962) 462
27) J. R. Huizenga and G. J. Igo, Argonne National Laboratory Report, ANL-6373 (1961) unpublished
28) D. Bodansky, Ann. Revs. Nucl. Sci. **12** (1962) 84
29) R. Hofstadter, Ann. Revs. Nucl. Sci. **7** (1957) 308
30) Daniel Sperber, Palmer Physical Laboratory, Princeton University, NYO-2961 (1961) unpublished
31) D. W. Lang, in Proc. Third Conf. on Reactions Between Complex Nuclei (University of California Press, Berkeley and Los Angeles, 1963) p. 248
32) T. Ericson, Advan. Phys. **36** (1960) 481
33) G. A. Pik-Pichak, JETP **38** (1960) 768; JETP (Soviet Physics) **11** (1960) 557